Short-range and long-range incommensurate magnetic ordering in the frustrated antiferromagnets $Ca_3Co_{2-x}Fe_xO_6$: A neutron diffraction study

Anil Jain and S. M. Yusuf*

Solid State Physics Division, Bhabha Atomic Research Centre, Mumbai 400085, India

(Received 8 September 2010; revised manuscript received 23 December 2010; published 25 May 2011)

We present the results of a detailed neutron powder diffraction study on the spin-chain compounds $Ca_3Co_{2-x}Fe_xO_6$ ($x=0.2$ and 0.4), crystallizing in the rhombohedral structure (space group $R\bar{3}c$), in the temperature range of 1.5–20 K. At low temperature, these compounds show a long-range magnetic ordering (LRO) with an incommensurate structure having an amplitude modulation of the moments along the crystallographic c axis. Our analysis also shows that a short-ranged spin-spin correlation along the c axis (incommensurate type such as that of the LRO), however, with a long-range spin-spin correlation in the ab plane, coexists with the LRO below the LRO temperature of 20 and 17 K for $x=0.2$ and 0.4 samples, respectively. The observed long-range as well as the short-range magnetic ordering can be described by a model of platelet-like-shaped magnetic crystallites, disorderly stacked along the crystallographic c direction. At 1.5 K, the LRO and short-range ordering (SRO) contribute in the magnetic phase in volume ratios of 13:7 and 3:2 for $x=0.2$ and $x=0.4$, respectively. The magnetic correlation lengths at 1.5 K for the LRO (ξ_{I}^{c}) and SRO (ξ_{II}^{c}) along the c axis are ~1027 and 60 Å for $x=0.2$, and 1021 and 47 Å for $x=0.4$, respectively. The relative contribution of the LRO and SRO in the magnetic phase remains constant down to 1.5 K (below transition temperature).

DOI: 10.1103/PhysRevB.83.184425 PACS number(s): 75.25.−j, 75.30.Kz, 75.50.Ee

I. INTRODUCTION

A_3MXO_6-type [A = Ca or Sr, and (M,X) = transition-metal ions] spin-chain compounds containing one-dimensional spin chains (ferromagnetic) that are arranged on a triangular lattice (Fig. 1) have recently received a lot of attention due to their extraordinary magnetic properties[1–30] such as order by disorder, spin liquid, multiferrocity, etc. These compounds crystallize in the K_4CdCl_6-type rhombohedral structure with space group $R\bar{3}c$ (No. 167; $Z=6$). $Ca_3Co_2O_6$ (Refs. 2 and 18) is one of the most studied compounds of this family in which both M and X sites are occupied by the same type of transition-metal ions. The spin chains in this compound, running along the crystallographic c axis, are made up of alternating face-sharing octahedra (CoO_6) and trigonal prism (CoO_6). Due to different crystalline electric fields,[9] trivalent Co ions at the octahedral (OCT) and trigonal prism (TP) sites are in low-spin ($S=0$) and high-spin ($S=2$) states, respectively. A steplike shape of the magnetization curve has been observed[8,25] in the dc magnetization study of this compound, which has been ascribed to the phenomenon of quantum tunneling of magnetization. In a recent neutron diffraction study, it was revealed that below 25 K, $Ca_3Co_2O_6$ orders magnetically with a modulated partially disordered antiferromagnetic structure.[23] In the same study, it was reported that below 21 K, the long-range magnetic order coexists with a short-range magnetic order and the volume of the material, exhibiting short-range order, increases at the expense of the long-range order. The estimated correlation length in the ab plane for the short-range order at 5 K was 180 Å.

In order to investigate the variation in the crystal structure and magnetic properties associated with 3d electron filling at octahedral/tetrahedral sites in $Ca_3Co_2O_6$ compound, we substituted cobalt with iron. In our earlier reports,[19,20] we studied the effects of iron substitution on the structural and magnetic properties of the compounds $Ca_3Co_{2-x}Fe_xO_6$ ($x=0$, 0.1, 0.2, and 0.4) using low-temperature neutron diffraction, x-ray powder diffraction, dc magnetization, and Mössbauer spectroscopy techniques. Magnetic properties of the compounds $Ca_3Co_{2-x}Fe_xO_6$ ($x \leqslant 0.1$) have also been investigated by other groups[17,18] using Mössbauer spectroscopy. Our neutron diffraction as well as Mössbauer studies[19] confirmed that Fe^{+3} ions were located at the trigonal prism site, 6a (0,0,1/4) in these compounds. In the Mössbauer study of the compound $Ca_3Co_{1.98}Fe_{0.02}O_6$, Kageyama *et al.*[17] observed that Fe spin behaves as an "isolated paramagnetic moment" in the ordered host spin system and there is no exchange interaction between Co and Fe spins. Based on the analysis of the Mössbauer spectra of the compounds $Ca_3Co_{2-x}Fe_xO_6$ ($x=0$, 0.02, 0.04, and 0.1), Arail *et al.*[18] reported that Fe^{3+} spin remains in the "paramagnetic state" in the ferromagnetically ordered chains below the magnetic ordering temperature of 23 K, indicating that Fe spins are scarcely coupled with the Co spins having strong Ising nature. The isolated electron state of Fe^{3+} with $g=2.00$ has also been observed in the ESR study of the compound $Ca_3Co_{1.98}Fe_{0.02}O_6$ by Kageyama *et al.*[31] In the dc-magnetization study of the compounds $Ca_3Co_{2-x}Fe_xO_6$ ($x=0.1$, 0.2, and 0.4),[19] we have observed that substitution of iron broke the ferromagnetically ordered linear spin chain along the crystallographic c axis and strengthened the interchain antiferromagnetic exchange interaction. All the above-mentioned features of the Fe-substituted compounds were ascribed to the different spin nature of the Fe^{3+} ions (Heisenberg) in comparison to the Co^{3+} ions (Ising).

In order to understand how the iron in the paramagnetic state[31] affects the spin structure, we have recently carried out a neutron powder diffraction study[24] of the compounds $Ca_3Co_{2-x}Fe_xO_6$ ($x=0.2$ and 0.4). We have observed that two different magnetic structures, (i) amplitude-modulated structure with a propagation vector $\mathbf{k}=(0,0,1)$ and (ii) partially disordered antiferromagnetic (PDA) structure, are able to fit the same neutron diffraction patterns because the Fourier coefficients for each solution only differ in a global phase factor that cannot be determined by the powder diffraction

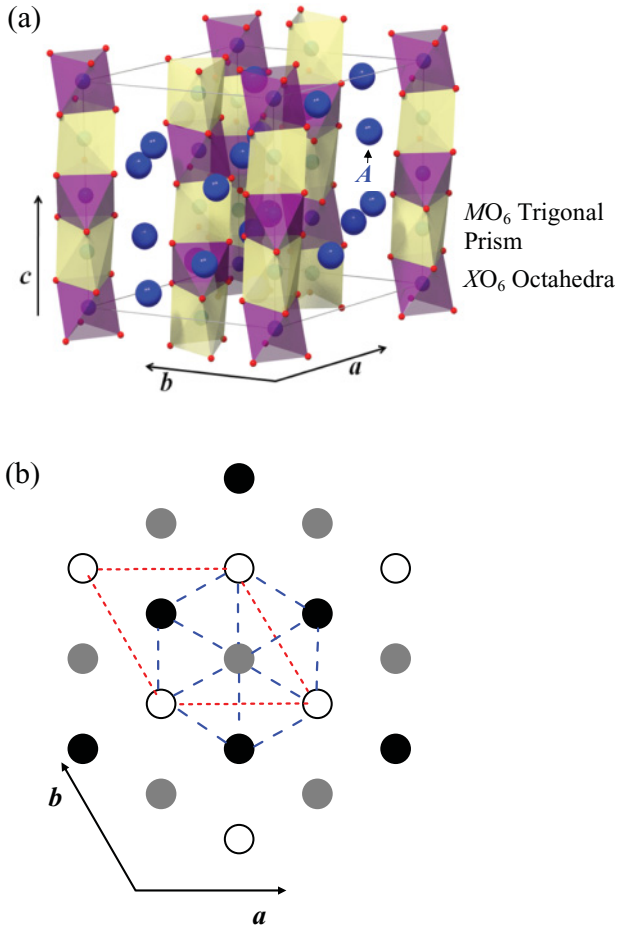

FIG. 1. (Color online) (a) Crystal structure of A_3MXO_6-type compounds. Atoms A and O are represented by blue (largest) and red (smallest) spheres, respectively. (b) A projection on the ab plane showing the triangular arrangement of spinchains. The black and white circles are spin-up and spin-down chains (made up of M/X atoms), respectively. The gray circles can be either in spin-up or spin-down states in the low-temperature phase or disordered chains in the high-temperature phase (partially disordered antiferromagnetic structure). The red short-dashed lines represent the unit cell.

experiment. A careful look at the observed neutron diffraction patterns reveals that a broad magnetic peak is always present along with the strongest antiferromagnetic Bragg peak observed at $Q \sim 0.79$ Å^{-1}. To understand the origin (whether it is due to frustration or due to the different nature of the spins in the chain) of the diffuse magnetic Bragg peaks for these Fe-substituted compounds, in the present study, we have made a very careful analysis of the neutron diffraction patterns below the long-range ordering temperature for $x = 0.2$ and 0.4 compounds. We address the question:what is the effect of iron (which is in the paramagnetic state) substitution on the magnetic correlation length for $x = 0.2$ and 0.4 compounds? Our detailed analysis reveals that the long-range magnetic ordering for these compounds is richer than the amplitude-modulated structure with a propagation vector $\mathbf{k} = (0,0,1)$ or a PDA structure, reported earlier.[24] It corresponds to an incommensurate structure with an amplitude modulation of the moments along the c axis. Our present analysis also reveals that the magnetic SRO coexists with the LRO well below the LRO temperature with a constant ratio of SRO and LRO intensities (down to 1.5 K). This observation (constant ratio of SRO and LRO intensities) is very much different from that for the parent compound $Ca_3Co_2O_6$, where the ratio changes with temperature. For $Ca_3Co_2O_6$, Agrestini *et al.* have observed finite correlation length in the ab plane for SRO. However, for the present Fe-substituted compounds, for SRO, we have observed finite correlation length along the c axis and long-range magnetic ordering in the ab plane. We also find that the correlation lengths for both short-range and long-range ordering do not differ very much with varying concentrations of Fe, indicating that Fe ions in a chain are located preferentially very close to each other. It therefore suggests that a higher concentration (for $x = 0.4$) of Fe hardly breaks the ferromagnetic bonds further as compared to that for the lower concentration of Fe (for $x = 0.2$). The results presented in this paper provide insight about the nature of magnetic ordering for the geometrically frustrated quasi-one-dimensional spin-chain compounds.

II. EXPERIMENTAL

Polycrystalline samples of the compounds $Ca_3Co_{2-x}Fe_xO_6$ ($x = 0.2$ and 0.4) were prepared by the conventional solid-state reaction method as described in our earlier paper.[19] Rietveld refinement of the room-temperature x-ray powder diffraction pattern confirmed the single phase formation of these compounds in the rhombohedral structure with space group $R\bar{3}c$ (No. 167; $Z = 6$). Neutron diffraction experiments were performed on the DMC (cold neutron powder diffractometer) at SINQ, Paul Scherrer Institute (PSI), Switzerland in the temperature range 1.5–20 K using a constant wavelength of 2.46 Å. The diffraction data were analyzed by the Rietveld refinement method using the FULLPROF (Ref. 32) program. The representation theory analysis was performed using the BASIREPS software.[32]

III. RESULTS AND DISCUSSION

Figures 2(a) and 2(b) depict temperature dependence of the neutron diffraction patterns for $x = 0.2$ and $x = 0.4$ compounds, respectively. Extra reflections appear in the diffraction patterns below ~20 and ~17 K for $x = 0.2$ and 0.4, respectively, which can be ascribed to the onset of an antiferromagnetic ordering. In the first approximation, the observed neutron powder diffraction patterns at 1.5 K can be fitted with two different magnetic structures: (i) PDA structure and (ii) amplitude-modulated structure with a propagation vector $\mathbf{k} = (0,0,1)$ as reported in our previous study.[24] The common point is that the net moment in the unit cell is zero for both magnetic structures. However, a careful inspection of the observed and calculated neutron diffraction patterns shows that the antiferromagnetic (AFM) Bragg peaks observed at $Q \sim 0.79$, 1.60, and 1.84 Å^{-1} are not well fitted by either of the above-mentioned two magnetic structures, as shown in Figs. 3(a), 3(b), 4(a), and 4(b). A detailed analysis of the neutron powder diffraction patterns at 1.5 K reveals that the magnetic structure is not commensurate, but it corresponds

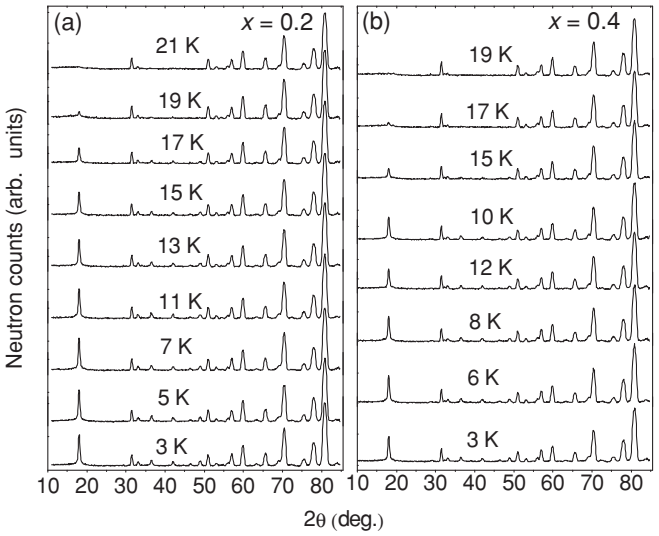

FIG. 2. Temperature evolution of the neutron powder diffraction patterns of the compounds (a) $Ca_3Co_{1.8}Fe_{0.2}O_6$ and (b) $Ca_3Co_{1.6}Fe_{0.4}O_6$. The additional peaks appear below 20 and 17 K for $Ca_3Co_{1.8}Fe_{0.2}O_6$ and $Ca_3Co_{1.6}Fe_{0.4}O_6$, respectively, due to the onset of an antiferromagnetic ordering.

to an incommensurate structure with propagation vector $\mathbf{k} = [0,0,1.0182(9)]$, as shown in Figs. 3(c) and 4(c).

We have determined the magnetic structure for this incommensurate structure, using the standard irreducible representational theory as described by Bertaut in Refs. 33 and 34.

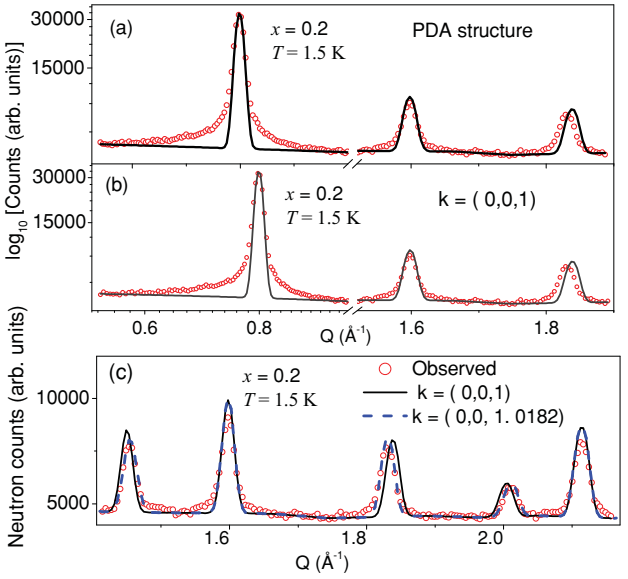

FIG. 3. (Color online) The Rietveld refined neutron powder diffraction patterns (only AFM peaks at $Q \sim 0.79$, 1.60, and 1.84 Å^{-1} are shown) for $Ca_3Co_{1.8}Fe_{0.2}O_6$ at 1.5 K using (a) the partially disordered antiferromagnet (PDA) structure and (b) the amplitude-modulated structure with ($\mathbf{k} =$ 0,0,1). (c) The Rietveld refined patterns for $Ca_3Co_{1.8}Fe_{0.2}O_6$ at 1.5 K are shown for two different values of the propagation vector $\mathbf{k} = (0,0,1)$ (solid line) and [0,0,1.0182(9)] (dashed line). On each plot, the open circles and solid line represent the experimental data points and the calculated diffraction pattern, respectively.

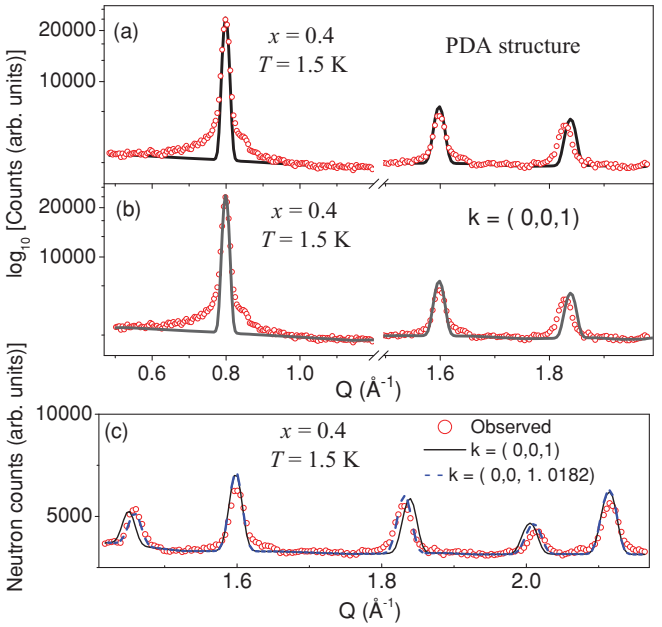

FIG. 4. (Color online) The Rietveld refined neutron powder diffraction patterns (only AFM peaks at $Q \sim 0.79$, 1.60, and 1.84 Å^{-1} are shown) for $Ca_3Co_{1.6}Fe_{0.4}O_6$ at 1.5 K using (a) the partially disordered antiferromagnet (PDA) structure and (b) the amplitude-modulated structure with ($\mathbf{k} =$ 0,0,1). (c) The Rietveld refined patterns for $Ca_3Co_{1.6}Fe_{0.4}O_6$ at 1.5 K are shown for two different values of the propagation vector $\mathbf{k} = (0,0,1)$ (solid line) and [0,0,1.0182(9)] (dashed line). On each plot, the open circles and solid line represent the experimental data points and the calculated diffraction pattern, respectively.

Symmetry analysis shows that the magnetic representation for 6*a* and 6*b* can be written as

$$\Gamma(6a) = 1\Gamma_1^{(1)} + 1\Gamma_2^{(1)} + 2\Gamma_3^{(0)}, \quad (1)$$

$$\Gamma(6b) = 1\Gamma_1^{(1)} + 1\Gamma_2^{(1)} + 2\Gamma_3^{(0)}. \quad (2)$$

Here, the representations Γ_1 and Γ_2 are one dimensional, while representation Γ_3 is two dimensional. The observed neutron powder diffraction patterns for these compounds cannot be fitted with the magnetic structure corresponding to the representations Γ_2 and Γ_3, whereas the magnetic structure corresponding to the representation Γ_1 is suitable to describe the observed neutron powder diffraction patterns. The magnetic structure belonging to the representation Γ_1 corresponds to a longitudinal amplitude-modulated structure (incommensurate), with a modulation and alignment of the moments along the crystallographic *c* axis as shown in Fig. 5. The magnetic moments at 6*a* (0,0,$\frac{1}{4}$) and 6*b* (0,0,0) sites are given by

$$\begin{aligned}\mathbf{m}_{L,\{j=6a,6b\}} &= \sum_{\{-\mathbf{K}+\mathbf{K}\}} \frac{1}{2}\mathbf{S}_j^{\mathbf{k}} \exp\{-2\pi i \mathbf{k}\cdot\mathbf{R}_L\} \\ &= \frac{1}{2}\left(\mathbf{S}_j^{\mathbf{k}} \exp\{-2\pi i \mathbf{k}\cdot\mathbf{R}_L\}\right. \\ &\quad \left. + \mathbf{S}_j^{-\mathbf{K}} \exp\{2\pi i \mathbf{k}\cdot\mathbf{R}_L\}\right) \\ &= \mathbf{S}_j^{\mathbf{k}} \cos\{2\pi \mathbf{k}\cdot\mathbf{R}_L\} \quad (3)\end{aligned}$$

Here $\mathbf{S}^{\mathbf{k}}_{6a}$ and $\mathbf{S}^{\mathbf{k}}_{6b}$, the Fourier coefficients, are the maximum magnetic moments at the 6*a* and 6*b* sites, respectively, and R_L is the translation vector with respect to the zeroth cell including the noninteger translations (inside the magnetic unit cell) *t*1 = (2/3,1/3,1/3) and *t*2 = (1/3,2/3,2/3). The observed and calculated neutron diffraction patterns (convoluted with the instrumental resolution function), corresponding to the representation Γ_1 with single magnetic correlation length, are shown in Figs. 6(a) and 7(a) for $x = 0.2$ and 0.4 samples, respectively. It is clear from Figs. 6(a) and 7(a) that the magnetic Bragg peak centered at $Q \sim 0.79$ Å^{-1} is broader [full width at half maximum (FWHM) = 0.489(2)° and 0.493(3)° for $x = 0.4$ and $x = 0.2$ compounds, respectively) than that expected (FWHM = 0.414° at $Q \sim 0.79$ Å^{-1}) from the instrumental resolution. In general, a broadening of Bragg reflections arises due to microstructure and/or magnetic domain size effects. In case of broadening due to microstructural effect, both nuclear and magnetic Bragg peaks are broadened, whereas domain size effect leads to a broadening of the magnetic Bragg peaks only. In the present study, we have observed that Bragg peaks of magnetic origin only are broadened. Therefore, for the present Fe-substituted compounds, magnetic domain size effect is responsible for the observed peak broadening.

To account for the magnetic domain size effect, domains of platelet-like shape are assumed. The size model No. 1 has been used to determine the magnetic structure (parameter IsizeModel = 1).[32] This model corresponds to a magnetic structure, for the representation Γ_1, in which a long-range magnetic ordering exists in the *ab* plane along with a finite spin-spin correlation length along the *c* direction (ξ^c). For this purpose, the Thompson-Cox-Hastings pseudo-Voigt function was used for the peak shape in the refinement.[32] This peak-shape function is a linear combination of Gaussian and Lorentzian peak-shape functions. The FWHM of Gaussian (H_G) and Lorentzian (H_L) components of the peak profile are given, respectively, by

$$H_G^2 = \left(U + D_{ST}^2\right)\tan^2\theta + \mathbf{V}\tan\theta + \mathbf{W} + \frac{I_G}{\cos^2\theta} \qquad (4)$$

and

$$H_L = X\tan^2\theta + \frac{Y + F(S_Z)}{\cos^2\theta}, \qquad (5)$$

where *U*, *V*, and *W* are the half width parameters characterizing the instrumental resolution function (IRF), D_{ST} is an anisotropic Gaussian contribution to microstrain, I_G is a Gaussian isotropic size parameter, *X* is a Lorentzian isotropic strain parameter, *Y* is a Lorentzian isotropic size parameter, and $F(S_z)$ is an anisotropic Lorentzian contribution arising from particle size. The functions D_{ST} and $F(S_z)$ have different expressions depending on the particular model used for the strain and size contributions to the broadening. The Rietveld refined neutron diffraction patterns using this model are shown in the insets of Figs. 6(b) and 7(b) for the $x = 0.2$ and $x = 0.4$ compounds, respectively. Here, single magnetic correlation length along the *c* axis is considered. However, agreement between the calculated and observed patterns is still not satisfactory.

In order to improve the refinement further, instead of the single magnetic correlation length along the *c* direction, we consider two different magnetic correlation lengths (ξ^c_{I} and ξ^c_{II}) along the *c* direction. As shown in Figs. 6(b) and 7(b), Rietveld refinement using such a model, with two different magnetic correlation lengths, satisfactorily described the observed neutron diffraction patterns at 1.5 K. For the $x = 0.2$ compound, the values of ξ^c_{I} and ξ^c_{II} at 1.5 K are ~1027 and 60 Å, respectively, whereas for the $x = 0.4$ sample, the values of ξ^c_{I} and ξ^c_{II} at 1.5 K are 1021 and 47 Å, respectively. The correlation lengths ξ^c_{I} and ξ^c_{II}, therefore, correspond to LRO and SRO, respectively. Here we would like to mention that the magnetic ordering in the *ab* plane is always long

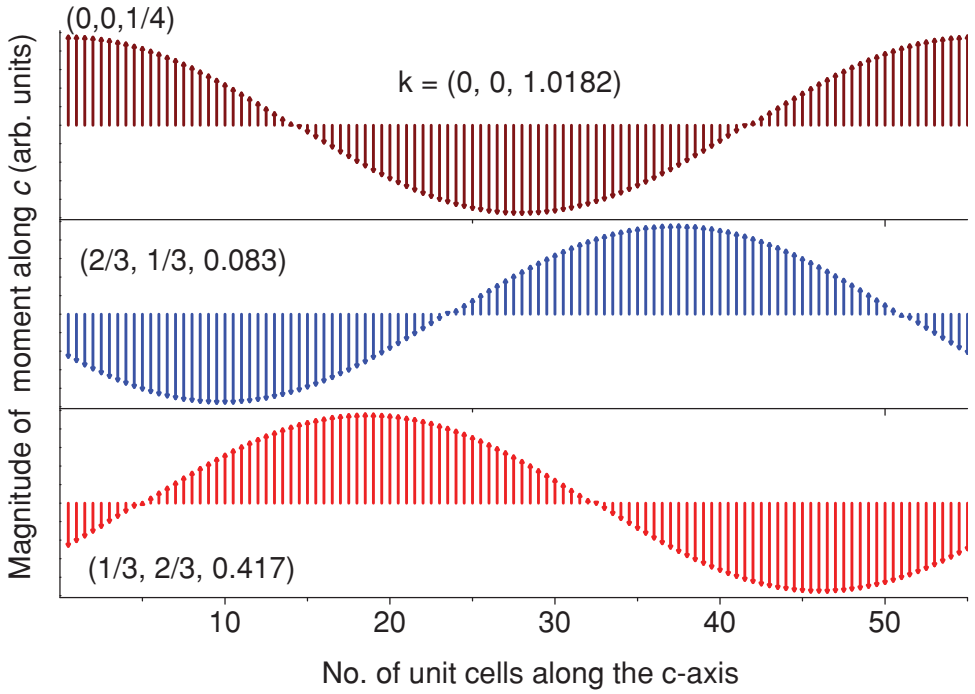

FIG. 5. (Color online) Schematic of the proposed longitudinal amplitude-modulated magnetic structure [incommensurate, $\mathbf{k} = \{0,0,1.0182\ (9)\}$] for 55 unit cells, with a modulation and alignment of the moments along the crystallographic *c* axis, corresponding to the model used to calculate the diffraction patterns shown in Figs. 3 and 4(c) for the $x = 0.2$ and 0.4 samples, respectively. The magnitude and direction of spins in the three adjacent spin chains with the (*x*, *y*) coordinate as (0,0), (2/3,1/3), and (1/3, 2/3) are shown. It can be viewed that the PDA structure (up- down- zero spin configuration in the neighboring spinchains) appears only at some specific lattice points.

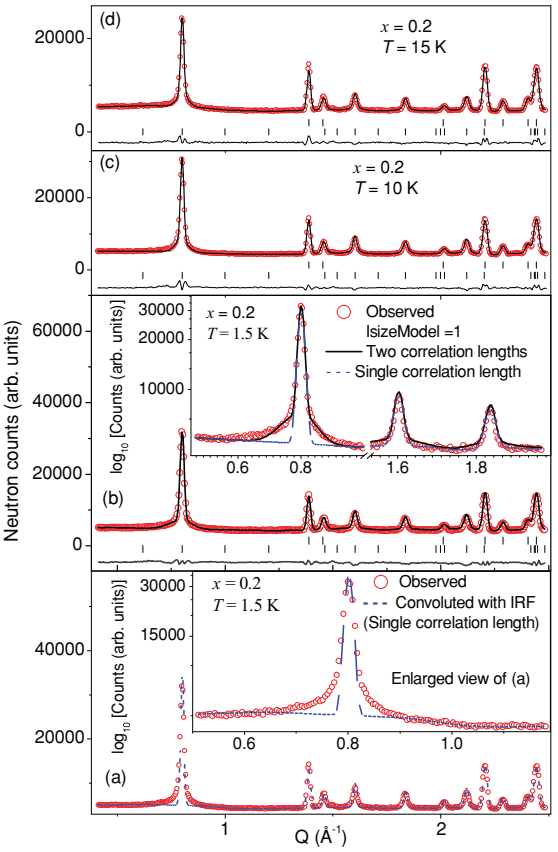

FIG. 6. (Color online) The Rietveld refined neutron powder diffraction patterns for $Ca_3Co_{1.8}Fe_{0.2}O_6$ corresponding to the representation Γ_1 of the incommensurate propagation vector $\mathbf{k} = [0,0,1.0182(9)]$ with (a) single correlation length at 1.5 K, convoluted with the instrumental resolution function (IRF), the inset (with neutron counts on a $\log_{10}$ scale) zooms in on the AFM peak at $Q \sim 0.79$ Å^{-1}, and (b) two correlation lengths at 1.5 K (with IsizeModel = 1 in the magnetic phase), the inset zooms in on the observed (open circles) and calculated patterns with both two correlation lengths (black solid line) and single correlation length (blue dashed line) using the IsizeModel = 1 over the selected Q range. The Rietveld refined patterns for $Ca_3Co_{1.8}Fe_{0.2}O_6$ with two magnetic correlation lengths at (c) 10 and (d) 15 K with IsizeModel = 1 as in (b). On each plot, the open circles and the solid/dashed line represent the experimental data points and the calculated diffraction patterns, respectively, and the difference is shown at the bottom as a solid line in (b), (c), and (d). The vertical marks correspond to the position of all allowed Bragg reflections for the crystal (top row) and magnetic (bottom row) reflections.

range for both LRO and SRO below their respective magnetic ordering temperatures (∼20 and ∼17 K for $x = 0.2$ and 0.4, respectively). The ratios of relative contributions of LRO (with correlation length ξ_{I}^{c}) and SRO (with correlation length ξ_{II}^{c}) to the magnetic Bragg peaks at 1.5 K are 13:7 and 3:2 for the $x = 0.2$ and $x = 0.4$ samples, respectively. For both compounds, the observed neutron powder diffraction patterns at all other temperatures (below their magnetic ordering temperatures), have been fitted with the same magnetic structure model [Figs. 6(c), 6(d), 7(c), and 7(d)]. The relative contribution of the LRO and SRO in the magnetic Bragg peaks also remains constant over the entire temperature range. Figures 8(a) and

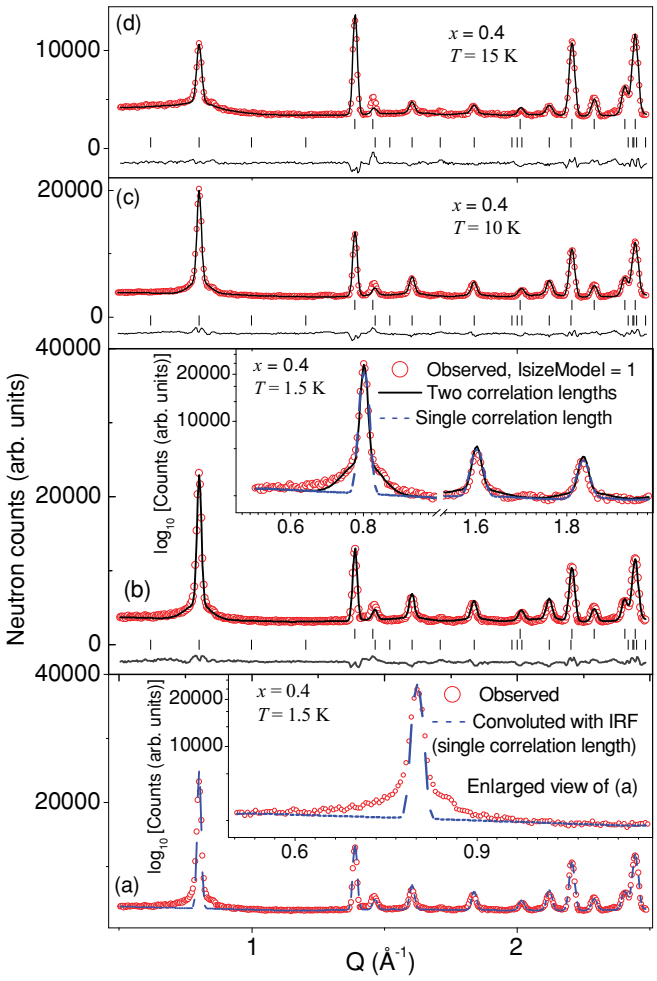

FIG. 7. (Color online) The Rietveld refined neutron powder diffraction patterns for $Ca_3Co_{1.6}Fe_{0.4}O_6$ corresponding to the representation Γ_1 of the incommensurate propagation vector $\mathbf{k} = [0,0,1.0182(9)]$ with (a) single correlation length at 1.5 K, convoluted with the instrumental resolution function (IRF), the inset (with neutron counts on a $\log_{10}$ scale) zooms in on the AFM peak at $Q \sim 0.79$ Å^{-1}, and (b) two correlation lengths at 1.5 K (with IsizeModel = 1 in the magnetic phase), the inset zooms in on the observed (open circles) and calculated patterns with both two correlation lengths (black solid line) and single correlation length (blue dashed line) using the IsizeModel = 1 over the selected Q range. The Rietveld refined patterns for $Ca_3Co_{1.6}Fe_{0.4}O_6$ with two magnetic correlation lengths at (c) 10 and (d) 15 K with IsizeModel = 1 as in (b). On each plot, the open circles and the solid/dashed line represent the experimental data points and the calculated diffraction patterns, respectively, and the difference is shown at the bottom as a solid line in (b), (c), and (d). The vertical marks correspond to the position of all allowed Bragg reflections for the crystal (top row) and magnetic (bottom row) reflections.

8(b) show the fitted profiles at various temperatures for the strongest magnetic Bragg peak at $Q = 0.79$ Å^{-1}. The derived temperature dependence of the magnetic correlation lengths ξ_{I}^{c}(LRO) and ξ_{II}^{c}(SRO) for both compounds is depicted in Figs. 8(c) and 8(d). It is evident that for both compounds, the correlation length ξ_{I}^{c}(LRO) decreases with increasing temperature, whereas the correlation length ξ_{II}^{c} (SRO) remains approximately constant for both compounds.

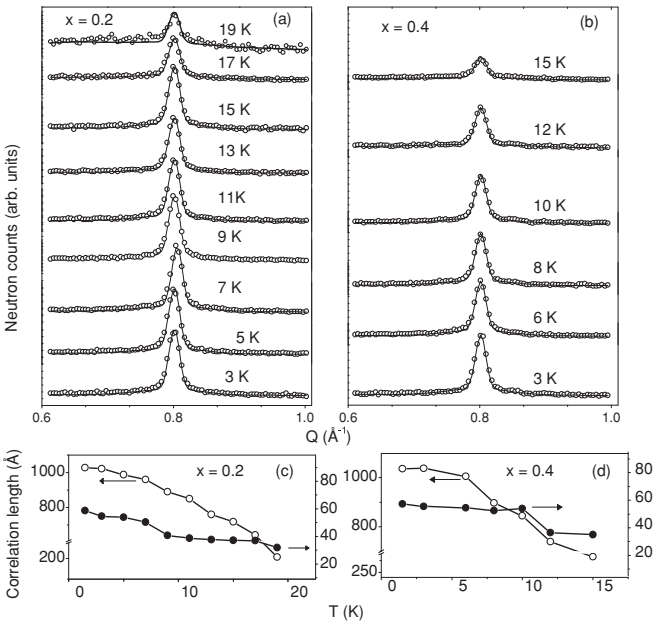

FIG. 8. Observed (open circles) and calculated (solid lines) patterns with parameter IsizeModel = 1 and two magnetic correlation lengths ξ_{I}^{c} and ξ_{II}^{c} at different temperatures for the strongest magnetic Bragg peak for (a) $x = 0.2$ (left top) and (b) 0.4 (right top) compounds. The variation of correlation lengths for LRO (ξ_{I}^{c}, open circle) and SRO (ξ_{II}^{c}, solid circle) for (c) $x = 0.2$ (left bottom) and (d) $x = 0.4$ (right bottom) compounds. Solid lines in (c) and (d) are guides to the eye.

The values of the maximum ordered magnetic moments $\mathbf{m}_{6a}$ and $\mathbf{m}_{6b}$ (at 1.5 K) for the $x = 0.2$ compound are $4.82(3)\mu_B$ per (6*a*) site and $0.04(2)\mu_B$ per (6*b*) site, respectively. For the $x = 0.4$ compound, these values are $5.11(2)\mu_B$ per (6*a*) site and $0.02(1)\mu_B$ per (6*b*) site. It is interesting to note that the values of the ordered magnetic moment $\mathbf{m}_{6a}$ ($4.82\mu_B$ and $5.11\mu_B$ for $x = 0.2$ and 0.4 compounds, respectively) are equal for LRO and SRO. The nearly zero value of the ordered magnetic moment for Co^{3+} ions at the 6*b* site (OCT site) may be ascribed to a stronger crystalline electric field.[19] For the 6*a* site, the observed values of the magnetic moments are higher than the theoretically calculated values derived using the expression $\mathbf{m}_6a = [(1-x)\mathbf{m}_{\mathrm{Co}} + x\mathbf{m}_{\mathrm{Fe}}]$. Here $\mathbf{m}_{\mathrm{Co}}$ and $\mathbf{m}_{\mathrm{Fe}}$ are the spin-only values of the ordered moment for Co^{3+} and Fe^{3+}, respectively. The theoretically expected ordered moment values with fully quenched orbital moment for $\mathbf{m}_{6a}$ are $4.2\mu_B$ per site and $4.4\mu_B$ per site for $x = 0.2$ and 0.4, respectively. A high value of the effective paramagnetic moment was also observed in our previous dc magnetization study ($5.72\mu_B$ and $5.97\mu_B$ for $x = 0.2$ and 0.4 compounds, respectively).[19] The observed high value of magnetic moment at the 6*a* site in these Fe-substituted compounds may be ascribed to the presence of an orbital moment for Co^{3+} ions. From magnetic dichroism measurements,[14] an orbital moment of $1.7\mu_B$ was reported for Co^{3+} ions at the 6*a* (TP) site for the compound $Ca_3Co_2O_6$.

Now we discuss the observed incommensurate amplitude-modulated structure and the coexistence of two correlation lengths ξ_{I}^{c} and ξ_{II}^{c} for the studied compounds $Ca_3Co_{2-x}Fe_xO_6$ ($x = 0.2$ and 0.4). In the structure of these compounds, each spin chain is surrounded by six chains, forming a triangular lattice in the *ab* plane [as shown in Fig. 1(b)]. The magnetic ions in the neighboring spin chains (in a triangular lattice) are shifted by 1/6 or 1/3 along the crystallographic *c* axis. In a triangular lattice, the spin configurations in the neighboring spin chains are up- down- down/zero. This kind of spin arrangement gives rise to a competition between ferromagnetic intrachain and antiferromagnetic interchain exchange interactions. These competing interactions give rise to a noncollinear spin arrangement if single ion anisotropy is weak. However, if the single-ion anisotropy is strong, these competing interactions may give rise to an incommensurate amplitude-modulated structure as observed for the present Fe-substituted compounds (Fig. 5). In the studied iron-substituted compounds, Fe^{3+} ($3d^5$) ions carry zero orbital moment, so it cannot have local Ising anisotropy in the presence of cubic crystalline field (Co^{3+} ions have local Ising anisotropy). Different spin characters of host (Ising, Co^{3+}) and impurity (Heisenberg, Fe^{3+}) spins has been observed in the Mössbauer[17,18] and ESR (Ref. 31) studies where Fe^{3+} ions remain in the paramagnetic state in the ferromagnetically ordered chains. The observed two correlation lengths in the present study also suggest that the iron spin (Heisenberg) breaks the ferromagnetic chains and its (Fe^{3+}) spin remains either in the paramagnetic state or freezes randomly (due to the competing exchange interactions) at low temperatures. No change in the ratio of intensity of the long-range and the short-range ordering also suggests that the magnetic ordering in the ferromagnetic chains is stable down to 1.5 K. We have also observed that the correlation lengths for both SRO and LRO do not differ much with varying concentrations of Fe. It is, therefore, evident that a higher concentration (for $x = 0.4$) of Fe hardly breaks the ferromagnetic bonds further as compared to that for the lower concentration of Fe (for $x = 0.2$). More than one spin-spin correlation length has been observed in the neutron diffraction studies of the other frustrated magnets $Tb_2Sn_2O_7$ (Ref. 35) and $LiMn_2O_4$ (Ref. 36).

For the parent compound $Ca_3Co_2O_6$, Agrestini *et al.*[23] have shown that the magnetic propagation vector $\mathbf{k} = (0,0,k_z \sim 1.01)$ is incommensurate with the crystal structure. They described the physical origin of modulation in the magnetic structure in terms of the competition between ferromagnetic intrachain (due to direct Co-Co overlap) and antiferromagnetic interchain exchange interactions. Agrestini *et al.* have fitted only the (100) magnetic Bragg peak using two Gaussian functions with significantly different widths, the narrower of which corresponds closely to the instrumental resolution. The broad Gaussian peak corresponds to the SRO. However, in the present study, we have carried out a detailed analysis of the neutron diffraction patterns and established the coexistence of LRO and SRO. Moreover, in our analysis, we have taken a wide *Q* range (magnetic Bragg peaks observed at $Q \sim 0.79$, 1.6029, 1.8365, 2.1204, and 2.6881 Å^{-1}), unlike in Ref. 23 where only the (100) magnetic Bragg peak was considered, to estimate the correlation lengths for SRO and LRO. For the compound $Ca_3Co_2O_6$, the estimated correlation length in the *ab* plane for the short-range order at 5 K is 180 Å (Ref. 23). However, for the present Fe-substituted compounds, a long-range magnetic ordering always exists in the *ab* plane. We have defined LRO and SRO based upon the extent of the correlation length along

the c axis. For the compound $Ca_3Co_2O_6$,[23] below 18 K, a reduction in the intensity of the strongest magnetic reflection (100) was observed in the powder as well as single crystal neutron diffraction studies. At 21 K, the ratio of intensity contribution of the short-range and the long-range magnetic ordering to the magnetic Bragg peaks is 0.2; this ratio increases to 0.7 at low temperatures. This indicates the instability of the long-range magnetic order at lower temperatures. For the present Fe-doped compounds, we have also observed a long-range as well as short-range magnetic ordering down to 1.5 K. However, we have not observed any reduction in the intensity of the strongest magnetic reflection (100) at $Q \sim 0.79$ Å^{-1}. The ratio of intensity of the long-range and the short-range ordering also remains constant down to 1.5 K. It is, therefore, evident that unlike for the compound $Ca_3Co_2O_6$, for the present Fe-doped compounds $Ca_3Co_{2-x}Fe_xO_6$, the short-range magnetic correlation does not grow at the expense of the long-range magnetic correlation.

Niitaka *et al.*,[29] based on the analysis of the neutron diffraction patterns, reported that compound Ca_3CoRhO_6 ordered magnetically below 100 K in a PDA state, in which 1/3 ferromagnetic spin chains (in a triangle) are spin up ($+M$), 1/3 ferromagnetic spin chains are spin down ($-M$), and the remaining 1/3 are incoherent (disordered). Below 30 K, the 1/3 incoherent spin chains freeze and give rise to a frozen PDA state. On the contrary, the magnetic structure of the present Fe-doped compounds is incommensurate with an amplitude modulation of the moments along the c axis, where the magnetic configuration of the neighboring spin chains (arranged in a triangle) is ($+M$,$-M$,0) at specific lattice points only (Fig. 5). This is different from the PDA state, where ($+M$,$-M$,0) structure is present for all lattice points. On the contrary, to the reported frozen-PDA state (below 30 K) for the compound Ca_3CoRhO_6, no phase transition has been observed at low temperature for the present Fe-doped compounds. Loewenhaupt *et al.*[28] also proposed the PDA state for the magnetic structure of the compound Ca_3CoRhO_6 below 100 K. In addition, they observed a diffuse magnetic peak, superimposed over the strongest magnetic Bragg peak (100) below as well as above the ordering temperature of 100 K. The estimated correlation lengths for the diffuse magnetic ordering above and below 100 K are 16 and 23 Å, respectively, indicating that with the establishment of the long-range magnetic ordering, the correlation length for diffuse magnetic scattering increases. The intensity of the diffuse magnetic peak increases with lowering of the temperature, reaching a maximum around 100–150 K, and then decreases at lower temperatures. The position of the diffuse magnetic peak shifts to a larger scattering angle with decreasing temperature. For the present Fe-doped compounds, a diffuse magnetic peak, superimposed over the strongest (sharper) magnetic Bragg peak, has been observed only below the long-range ordering temperature. Here the relative contribution of LRO and diffuse magnetic scattering (SRO) in the magnetic phase remains

TABLE I. Magnetic structures of the compounds of the A_3MXO_6 family (determined from neutron diffraction studies)

Properties	Compounds			
	$Ca_3Co_2O_6$	Ca_3CoRhO_6	Sr_3HoCrO_6	$Ca_3Co_{2-x}Fe_xO_6$
T_N (K)	25	100 (T_{N1}) 30 (T_{N2})	15	20 ($x = 0.2$) 17 ($x = 0.4$)
Magnetic structure	Modulated PDA structure with $\mathbf{k} = (0,0,1.01)$	PDA (30 K $\leqslant T \leqslant$ 100 K) Frozen-PDA ($T \leqslant$ 30 K)	PDA	Modulated structure with K = [0,0,1.0182(9)]
Temperature dependence of intensity of the magnetic reflection (100)	Below 18 K, intensity decreases with decreasing temperature	Increases with decreasing temperature (below T_{N1}) and then constant below 30 K	Below 9 K, intensity decreases with decreasing temperature	Below T_N, increases with decreasing temperature
Coexistence of short-range and long-range ordering	Below 21 K	Above as well as below T_{N1}	Below T_N	Below T_N
Ratio of intensity contribution from short-range and long-range	0.2 at 21 K 0.7 at 5 K	Not reported	Not reported	0.54 ($x = 0.2$) and 0.67 ($x = 0.4$) Remains constant below T_N
Correlation lengths	180 Å for SRO (at 5 K)	16 Å ($T \geqslant$ 100 K) for SRO 6.415 Å at 3 K (SRO)	400 Å for LRO (at 9 K) 40 Å for SRO (at 9 K)	1027 Å (LRO) and 60 Å (SRO) along c axis at 1.5 K ($x = 0.2$). For both cases, LRO in the ab plane. 1021 Å (LRO) and 47 Å (SRO) along (c axis at 1.5 K ($x = 0.4$). For both cases, LRO in the ab plane
References	23	28,29	37	Present study

constant (below transition temperature) down to 1.5 K with no change in the position of the diffuse magnetic peak. Besides, the correlation length, corresponding to the diffuse magnetic scattering for the present Fe-doped compounds, also remains approximately constant below the long-range magnetic ordering temperature. It is therefore evident that the substitution of the Ising Co spins by the Heisenberg Fe spins stabilizes the incommensurate amplitude-modulated magnetic phase over the entire temperature range.

The low-temperature neutron diffraction study for the compound Sr_3HoCrO_6 was carried out by Hardy *et al.*[37] The extra peaks in the neutron diffraction patterns have been observed below 15 K. Vardy *et al.* have proposed the PDA state for the magnetic structure of this compound. The magnetic short-range ordering coexists with the long-range ordering below the long-range ordering temperature (15 K). A decrease in the correlation length with decreasing temperature from 9 to 1.5 K has been observed for long-range ordering. Moreover, a high background in the small-angle part of the neutron diffraction patterns has been observed at temperatures above as well as below the long-range ordering temperature (10 K), the reason of which is not reported. In sharp contrast, the LRO correlation length for the present Fe-substituted compounds increases with decreasing temperature. The coexistence of the long-range and the short-range magnetic order for the compound Sr_3HoCrO_6 is similar to the present Fe-doped compounds. However, as mentioned earlier, the observed PDA structure for the compound Sr_3HoCrO_6 is very much different from the observed amplitude-modulated incommensurate structure for the present Fe-substituted compounds. It is therefore clear that the magnetic correlations for the present Fe-doped compounds are very much different from the compound Sr_3HoCrO_6, except a coexistence of the long-range and the short-range order. The magnetic structures of the present Fe-doped compounds are significantly different than those for the compounds $Ca_3Co_2O_6$ and Ca_3CoRhO_6 as well, despite the fact that all these spin-chain compounds crystallize in the rhombohedral structure with space group $R\bar{3}c$. A comparison of the magnetic structures of the compounds of the A_3MXO_6 family is given in Table I.

IV. SUMMARY AND CONCLUSION

The magnetic structure of the spin-chain compounds $Ca_3Co_{2-x}Fe_xO_6$ ($x = 0.2$ and 0.4) has been investigated by neutron powder diffraction experiments. The Rietveld refinement of neutron diffraction patterns confirmed a coexistence of short-range and long-range incommensurate magnetic structures with an amplitude modulation of the moments along the c axis, below ~20 and ~17 K for $x = 0.2$ and 0.4, respectively. A model of platelet-like-shaped magnetic crystallites, disorderly stacked along crystallographic c direction [Isize model = 1 in FULLPROF], describes the observed magnetic short-range as well as the long-range order satisfactorily. The maximum values of ordered magnetic moments at the 6*a* site (at 1.5 K) are $4.82\mu_B$ and $5.11\mu_B$ for $x = 0.2$ and 0.4 compounds, respectively. The same values of the ordered magnetic moment ($4.82\mu_B$ and $5.11\mu_B$ for $x = 0.2$ and 0.4 compounds, respectively) are observed for both LRO and SRO. The nearly zero value of the ordered moment has been observed for the 6*b* site for both compounds. The magnetic correlation lengths along the c axis, at 1.5 K, for the LRO (ξ_I^c) and SRO (ξ_{II}^c) are ~1027 and 60 Å for the compound $x = 0.2$; and 1021 and 47 Å for the compound $x = 0.4$, respectively. For both compounds, the magnetic correlation length for the LRO increases with decreasing temperature, while for the SRO, it remains approximately constant down to 1.5 K. The relative contributions of the LRO and SRO in the magnetic Bragg peaks are in the ratio of 13:7 and 3:2 for $x = 0.2$ and $x = 0.4$, respectively. This ratio remains unchanged down to 1.5 K for both compounds, indicating that the volume fractions of the compound exhibiting the short-range order and long-range order remain constant. The coexistence of SRO and LRO incommensurate magnetic structures can be a good model to understand the spin-spin correlations for other compounds of the A_3MXO_6 family, especially for the compounds Ca_3CoRhO_6 (Refs. 28 and 29) and Sr_3HoCrO_6 (Ref. 37). The present results are very interesting for the quasi-one-dimensional spin-chain compounds of the family A_3MXO_6 and would encourage the scientific community to investigate the magnetic structure of the other compounds of the A_3MXO_6 family. A single crystal neutron diffraction study will be of great help to provide further insight on the microscopic nature of the magnetic ordering in these compounds.

ACKNOWLEDGMENTS

This work is based on experiments performed at the Swiss spallation neutron source SINQ, Paul Scherrer Institute, Villigen, Switzerland. The authors would like to acknowledge the help received from L. Keller in performing the neutron diffraction experiments. The authors are grateful to Juan Rodriguez Carvajal for his help in the refinement of neutron diffraction data.

*Corresponding author: smyusuf@barc.gov.in

[1] K. E. Stitzer, J. Darriet, and H.-C. zur Loye, Curr. Opin. Solid State Mater. Sci. **5**, 535 (2001).
[2] S. Aasland, H. Fjellvåg, and B. Hauback, Solid State Commun. **101**, 187 (1997).
[3] H. Kageyama, K. Yoshimura, K. Kosuge, M. Azuma, M. Takano, H. Mitamura, and T. Goto, J. Phys. Soc. Jpn. **66**, 3996 (1997).
[4] V. Hardy, S. Lambert, M. R. Lees, and D. McK. Paul, Phys. Rev. B **68**, 014424 (2003).
[5] B. Martínez, V. Laukhin, M. Hernando, J. Fontcuberta, M. Parras, and J. M. González-Calbet, Phys. Rev. B **64**, 012417 (2001).
[6] B. Raquet, M. N. Baibich, J. M. Broto, H. Rakoto, S. Lambert, and A. Maignan, Phys. Rev. B **65**, 104442 (2002).
[7] S. Majumdar, V. Hardy, M. R. Lees, D. McK. Paul, H. Rousselière, and D. Grebille, Phys. Rev. B **69**, 024405 (2004).

[8] V. Hardy, M. R. Lees, O. A. Petrenko, D. McK. Paul, D. Flahaut, S. Hébert, and A. Maignan, Phys. Rev. B **70**, 064424 (2004).
[9] E. V. Sampathkumaran, N. Fujiwara, S. Rayaprol, P. K. Madhu, and Y. Uwatoko, Phys. Rev. B **70**, 014437 (2004).
[10] R. Frésard, C. Laschinger, T. Kopp, and V. Eyert, Phys. Rev. B **69**, 140405(R) (2004).
[11] V. Hardy, D. Flahaut, M. R. Lees, and O. A. Petrenko, Phys. Rev. B **70**, 214439 (2004).
[12] J. Sugiyama, H. Nozaki, J. H. Brewer, E. J. Ansaldo, T. Takami, H. Ikuta, and U. Mizutani, Phys. Rev. B **72**, 064418 (2005).
[13] K. Takubo, T. Mizokawa, S. Hirata, J.-Y. Son, A. Fujimori, D. Topwal, D. D. Sarma, S. Rayaprol, and E.-V. Sampathkumaran, Phys. Rev. B **71**, 073406 (2005).
[14] T. Burnus, Z. Hu, M. W. Haverkort, J. C. Cezar, D. Flahaut, V. Hardy, A. Maignan, N. B. Brookes, A. Tanaka, H. H. Hsieh, H.-J. Lin, C. T. Chen, and L. H. Tjeng, Phys. Rev. B **74**, 245111 (2006).
[15] O. A. Petrenko, J. Wooldridge, M. R. Lees, P. Manuel, and V. Hardy, Eur. Phys. J. B **47,** 79 (2005).
[16] H. Kageyama, K. Yoshimura, K. Kosuge, X. Xu, and S. Kawano, J. Phys. Soc. Jpn. **67**, 357 (1998).
[17] H. Kageyama, S. Kawasaki, K. Mibu, M. Takano, K. Yoshimura, and K. Kosuge, Phys. Rev. Lett. **79**, 3258 (1997).
[18] J. Arai, H. Shinmen, S. Takeshita, and T. Goko, J. Magn. Magn. Mater. **272-276**, 809 (2004).
[19] A. Jain, S. Singh, and S. M. Yusuf, Phys. Rev. B **74**, 174419 (2006).
[20] I. Nowik, A. Jain, S. M. Yusuf, and J. V. Yakhmi, Phys. Rev. B **77**, 054403(2008).
[21] S. Takeshita, J. Arai, T. Goko, K. Nishiyama, and K. Nagamine, J. Phys. Soc. Jpn. **75**, 034712 (2006).
[22] H. Kageyama, K. Yoshimura, K. Kosuge, H. Mitamura, and T. Goto, J. Phys. Soc. Jpn. **66**, 1607 (1997).
[23] S. Agrestini, L. C. Chapon, A. Daoud-Aladine, J. Schefer, A. Gukasov, C. Mazzoli, M. R. Lees, and O. A. Petrenko, Phys. Rev. Lett. **101**, 097207 (2008)
[24] A. Jain, S. M. Yusuf, J. Campo, and L. Keller, Phys. Rev. B **79**, 184428 (2009).
[25] A. Maignan, V. Hardy, S. Hébert, M. Drillon, M. R. Lees, O. Petrenko, D. McK. Paul, and D. Khomskii, J. Mater. Chem. **14**, 1231 (2004).
[26] N. Bellido, C. Simon, and A. Maignan, Phys. Rev. B **77**, 054430 (2008).
[27] S. Agrestini, C. Mazzoli, A. Bombardi, and M. R. Lees, Phys. Rev. B **77**, 140403(R) (2008).
[28] M. Loewenhaupt, W. Schäfer, A. Niazi, and E. V. Sampathkumaran, Eurphys. Lett. **63**, 374 (2003).
[29] S. Niitaka, K. Yoshimura, K. Kosuge, M. Nishi, and K. Kakurai, Phys. Rev. Lett. **87**, 177202 (2001).
[30] S. Niitaka, H. Kageyama, K. Yoshimura, K. Kosuge, S. Kawano, N. Aso, A. Mitsuda, H. Mitamura, and T. Goto J. Phys. Soc. Jpn. **70**, 1222 (2001).
[31] H. Kageyama, K. Yoshimura, K. Kosuge, H. Nojiri, K. Owari, and M. Motokawa, Phys. Rev. B **58**, 11150 (1998)
[32] J. Rodriguez-Carvajal, Physica B **192**, 55 (1993).
[33] E. F. Bertaut, *Spin Configurations in Ionic Structures: Theory and Practice, in Magnetism*, edited by G. T. Rado and H. Suhl (Academic, New York, 1963), Vol. 3.
[34] E. F. Bertaut, Acta Crystallogr., Sect. A: Cryst. Phys. Diffr. Theor. Gen. Crystallogr. **24**, 217 (1968).
[35] I. Mirebeau, H. Mutka, P. Bonville, A. Apetrei, and A. Forget, Phys. Rev. B **78**, 174416 (2008).
[36] J. E. Greedan, C. R. Wiebe, A. S. Wills, and J. R. Stewart, Phys. Rev. B **65**, 184424 (2002).
[37] V. Hardy, C. Martin, G. Martinet, and G. André, Phys. Rev. B **74**, 064413 (2006).